Fast determination of phases in LiFePO4 using low losses in electron energy-loss spectroscopy

Philippe Moreau, Vincent Mauchamp, Florent Boucher

Fast determination of phases in $LiFePO_4$ using low losses in electron energy-loss spectroscopy

P. Moreau[1], V. Mauchamp[2], and F. Boucher[1]

[1]*Institut des Matériaux Jean Rouxel (IMN), Université de Nantes, CNRS, 2, rue de la Houssinière, BP32229, 44322 Nantes Cedex 3, France*

[2]*PhyMAT (ex LMP) SP2MI – Boulevard 3, Téléport 2 – BP 30179 - 86962 Futuroscope, Chasseneuil Cedex, France*

Experimental valence electron energy loss spectra (VEELS), up to the Li K edge, obtained on different phases of Li_xFePO_4 are compared to first principles calculations using the density functional code WIEN2k. In the 4-7 eV range, a large peak is identified in the $FePO_4$ spectrum, but is absent in $LiFePO_4$, which could allow the easy formation of energy filtered images. The intensity of this peak, non sensitive to the precise orientation of the crystal, is large enough to rapidly determine existing phases in the sample and permit future dynamical studies. Solid solution and two-phases regions are also differentiated using Fe $M_{2,3}$ / Li K edges.

Rechargeable lithium batteries are of considerable technological interest in the field of portable electronic devices and will soon be the standard electrical storage system in hybrid or all-electric vehicles.[1] Among positive electrode materials, lithium iron phosphate $LiFePO_4$ is one of the most promising. It is cheap, non toxic and shows excellent cycling properties when particles are coated with a carbon layer. Even if this coating and the utilization of nanosized particles clearly compensates for its intrinsic poor electronic conductivity, the precise microscopic processes at work inside the crystals are still being debated.[2-5] Given the crucial role of defects, interfaces, surfaces and local amorphous regions, the relevant phenomena are at the nanometer scale. They also involve very short time scales, due to the metastable nature of some phases and the remarkable high power performance of this material. In order to get a better insight into the electrochemical process, a local and fast method of analysis is thus necessary. In positive lithium battery materials, electron diffraction or high resolution transmission electron microscopy (HRTEM) have been used to determine local structures.[4, 6-11] Although these techniques can meet the spatial resolution requirement, they both have very time consuming limitations: electron diffraction necessitates the orientation of each crystal and HRTEM demands supporting image simulation. Local phases can also be obtained from core losses in electron energy-loss spectroscopy (EELS).[12, 13] The Fe $L_{2,3}$ edge has been used to characterize intercalated/deintercalated phases in Li_xFePO_4 grains,[2, 14] and analyze the phase front.[2] Nevertheless, using a Hartree-Slater model, the cross section for the Fe $L_{2,3}$ edge (situated around 708 eV) can be shown to be 30 times smaller than that of the Fe $M_{2,3}$ edge (around 54 eV).[15] Miao *et al*. published a study on that precise edge but the energy resolution was too poor to give any insight on the chemical process.[14] Valence EELS (VEELS), hence losses below 40 eV, is even more interesting since its intensity is approximately 10 times more intense than that of the $M_{2,3}$ edge. Such intensity could help meet the time scale criteria in order to both perform kinetic studies and limit electron beam damage.

In this paper, thanks to first principles calculations of dielectric functions, we analyze the usefulness of VEELS in determining local Li_xFePO_4 phases. We show that this method is fast and non sensitive to specimen orientation. With high enough energy resolution, solid solution and two-phases domains can also be identified by carefully examining Li-K /Fe M edges.

In order to validate the relevance of comparing experimental spectra with theoretical calculations, we first present, in Fig. 1(a) and Fig. 1(b), results for $FePO_4$ (FP) and $LiFePO_4$ (LFP), respectively. Calculations were performed with WIEN2k,[16] a full potential code, based on the density functional theory (DFT). Augmented plane wave plus local orbitals (APW+LO) basis sets were used for the self consistent field calculations. In order to take into account local magnetic moments on Fe^{II} (LFP) and Fe^{III} (FP) sites, spin polarized calculations were necessary. As previously done by Zhou *et al.*,[17] an antiferromagnetic (AF) order (AF along the channel **b** direction but ferromagnetic in the two others) was introduced together with the use of GGA+U approximation, considering a mean U_{eff} value (4.3 eV) for both LFP and FP. Dielectric functions were obtained in the optic approximation (q = 0).[18] Atomic coordinates were taken from Delacourt *et al.*[19] and details of the calculations are given in Ref. 20.[20] Analyzed samples were synthesized by the nitrate method,[21] so that no carbon coating, which could modify intensities in the VEELS region, was present. Chemically delithiated compounds were obtained by using proper amounts of NO_2BF_4.[2] Other experiments, performed on LFP crystals prepared with a carbon coating,[22] lead in fact to very similar results. Experiments were carried out on a H2000 Hitachi cold field emission gun TEM operated at 100 kV and always at liquid nitrogen temperature to avoid beam damages. Incident and collection angles were 1.4 mrad and 4.55 mrad, respectively. The probe size was around 60 nm in diameter, in order to avoid once again beam damages, which are especially large in the case of FP. A modified Gatan 666 spectrometer was used giving a 0.65 eV energy resolution at a 0.05eV/pixel dispersion.[23] VEELS were acquired in less than 0.2 s total time and Li K edges in around 5 s total time. Experimental spectra were gain, dark count, zero loss (ZL) and plural scattering corrected using the PEELS program.[24] In Fig. 1(a-b), the intensity scale (eV^{-1}) is common to both experimental and theoretical spectra. Experimental intensity was normalized to the ZL intensity and to the dispersion.[25] Theoretical spectra were obtained by introducing the dielectric functions into a formula first published by Wessjohann [26] and modified by Moreau *et al*. to take into account convergence and collection angles.[27] The thicknesses included in the calculations (444 Å for FP and 960 Å for LFP) were obtained from measurements of t/λ and estimates of λ using formulae given by Egerton.[28] The method was proven to give very reasonable results for various compounds.[27, 29] It is well known that within the framework of DFT, accurate band gaps are not provided due to the wrong treatment of self-energy effects.[30] Scissors operators corresponding to upwards energy shifts of 1 eV and 2 eV were consequently used for FP and LFP, respectively. In the case of FP, the three main contributions in the 4-8 eV range are well reproduced, as well as the shoulder around 13 eV and the overall shape of the plasmon peak. The plasmon peak is calculated 1.5 eV higher in energy (25 eV) compared to experiment. Since the plasmon

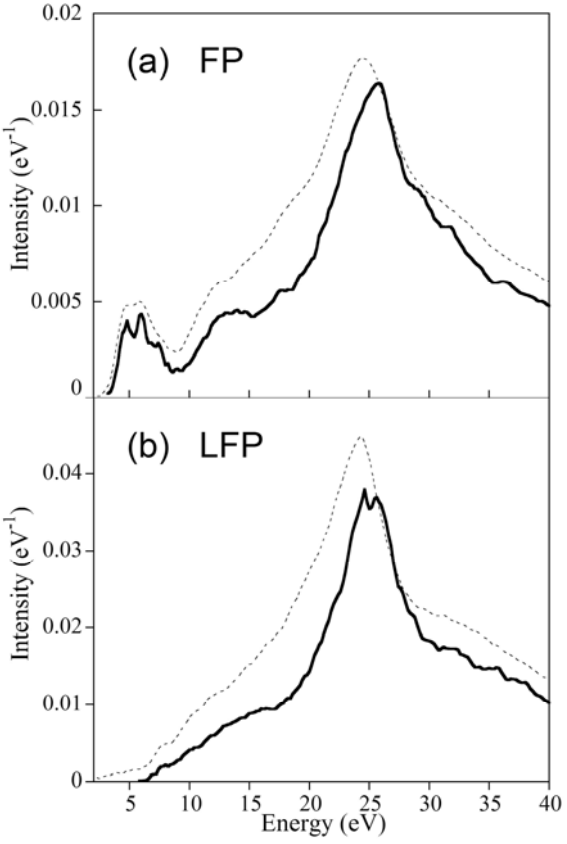

FIG. 1. (a) VEELS spectra for $FePO_4$. Thin dashed line: experiment; thick line: calculation. (b) VEELS spectra for $LiFePO_4$. Thin dashed line: experiment; thick line: calculation.

position is not sensitive to the choice of U_{eff}, excitonic effects and/or the q dependency of the dielectric functions (both not included in the present calculations) might be responsible for this discrepancy and will be evaluated in a forthcoming study. In the case of LFP, apart from the plasmon peak position, the agreement is also good. The small peak at 8 eV, the slowly varying intensity rise from 10 to 17 eV and the overall shape of the plasmon up to 40 eV are well reproduced.

From these results, it is very clear that VEELS spectra for both compounds are very dissimilar below 8 eV. Energy filtered TEM has long been demonstrated to allow mapping of local physical properties.[31, 32] By selecting electrons in the 4-5 eV range, energy filtered images with a high contrast between intercalated and non intercalated crystals could be obtained (90 % intensity change in this region). A direct phase imaging, without data processing such as three windows extraction or jump ratio, would thus be viable. Since spectrum intensity is quite high, such images could be obtained within tens of seconds with limited noise, allowing a dynamical approach of the intercalation process.

In order to prove that this method can also be applied whatever the crystal orientation is, calculated energy loss functions (ELF) for the different orientations are presented in Fig. 2 for FP. Anisotropy is small in the energy region presented and even smaller at higher energies. In particular, since the peak in the 4-7 eV region corresponds to transitions into levels with a *d* symmetry, this peak is observed in the three directions. The y direction can however be considered to slightly differ from the other two directions, especially with shoulders at 7 and 11 eV. In the AF $P2_1ma$ space group description of the FP structure, the y direction (**b** crystallographic axis) corresponds to the empty channels that lithium atoms fill in the $LiFePO_4$ phase. Since spectra in x and z directions are very similar, an average of the dielectric functions along these directions were considered in the simulations presented in Fig. 1. This averaged along with the y dielectric function was introduced in Wessjohann's formula (Fig. 1), which is in fact only valid for uniaxial crystals.[26]

The distinction between LFP and FP phases using energy filtered VEELS is thus straight forward, fast and not sensitive to crystal orientation.

In theory, VEELS could also be useful to identify a neat interface between fully intercalated and deintercalated phases, or Li_xFePO_4 single phase regions.[3, 5] We present experimental [Fig. 3(a)] and theoretical [Fig. 3(b)] spectra for a single phase sample and for a sample where both LFP and FP phases are present. The two-phases $Li_{0.6}FePO_4$ powder was obtained by chemical delithiation using a proper amount of NO_2BF_4. The single phase sample was obtained by rapid quenching in water of this same $Li_{0.6}FePO_4$ powder from 300°C.[14] In order to simulate an intermediate composition, the geometry of a supercell corresponding to the $Li_{0.5}FePO_4$ composition was optimized using the VASP program.[33] Experimental cell parameters were taken from Ref. 19 and optimized atomic parameters of this structure are given in Ref. 34.[34] In order to take into account the average half filling of lithium sites, various structural hypotheses were tested by lowering the symmetry. The atomic arrangement presenting the less stress corresponds to lithium ordering in the space group P11a and a charge ordering on the metal sites with a succession of Fe^{II} (**a**, **c**) planes and Fe^{III} (**a**, **c**) planes. A ferrimagnetic ordering was found to be the most stable magnetic configuration (AF coupling along the **b** axis).

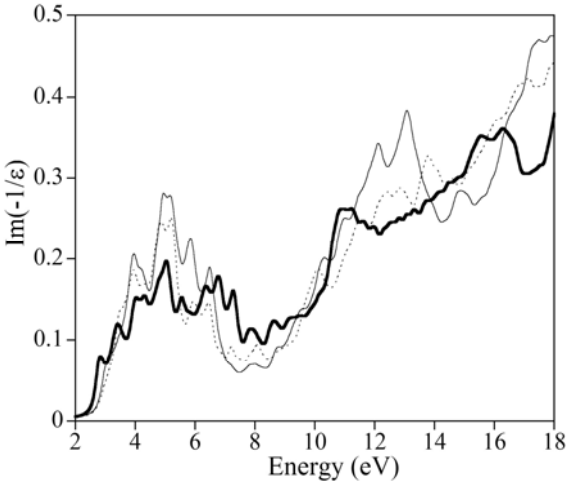

FIG. 2. Calculated anisotropic energy loss functions for $FePO_4$. Thin line: along the x direction; thick line: along the y direction; dashed line: along the z direction.

The same U_{eff} as for LFP was used. The optimized structure was then included in WIEN2k to obtain the dielectric functions for this compound.

Since 1 and 2 eV scissors operators were included to fit experiments in Fig. 1, an arbitrary 1.5 eV upward shift for $Li_{0.5}FePO_4$ (single phase) was used. The simulated ELF for a two-phases mixture (50% FP/ 50% LFP) was simply obtained by averaging the shifted ELF for FP and LFP. These simulations show that VEELS spectra for single phase and two-phases models are in fact very similar. Moreover, in the case of the two-phases situation, a contribution of the interface plasmon should be added.[28] An approximated calculation of this contribution, using the formula $Im(-1/(\varepsilon_{LP}+\varepsilon_{LFP}))$,[28] shows that it is somehow intermediate between the single phase and the two-phases spectra, hence complicating even further the interpretations. However, these results also mean that the 4-7 eV peak is roughly proportional to the lithium content in Li_xFePO_4 and could be used for a local quantification of lithium.

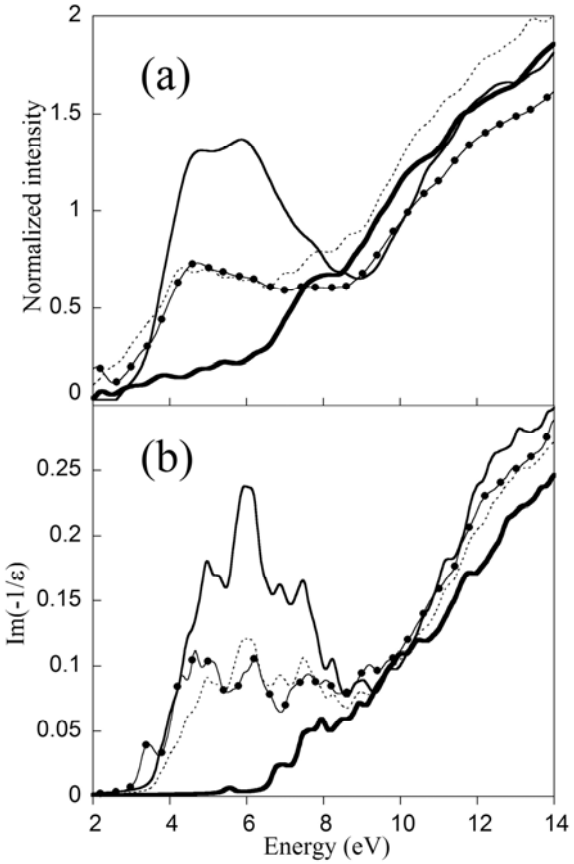

FIG. 3. (a) Experimental VEELS spectra. Normalized at 50 eV. (b) calculated VEELS spectra. Shifted according to Fig. 1 shifts. Thick line: $LiFePO_4$; dashed line: two-phases; thin line with dots: single phase; thin line: $FePO_4$.

Experimental results [Fig. 3(a)] confirm that it is impossible to safely discriminate between single and two-phases samples. It must also be pointed out that the two-phases spectrum was obtained in a region where two crystals were clearly on top of each other. Most crystals in the two-phases $Li_{0.6}FePO_4$ powder were indeed either fully or not at all deintercalated. The results are thus different from those presented by Laffont *et al.*[2] but merely illustrate the complex behavior of this system and the important role of kinetics.[5]

Since our instrumental resolution is twice as good as that utilized by Miao *et al.*,[14] we present detailed experiment/theory comparisons in the Fe $M_{2,3}$ edge/ Li K edge region (Fig. 4). Scissors operators for the calculated spectra were the same as those utilized for the VEELS spectra. In order to make the varying part of the spectra more obvious, a typical E^{-r} background was subtracted from both experimental and theoretical spectra. Let us first focus on FP (thin line) and LFP (thick line) experimental spectra. In the energy range presented [Fig. 4(a)], a single strong peak is obtained experimentally for FP at 58.1(2) eV. The peaks at 60.3(2), 61.6(2) and 64.3(2) eV for LFP are thus most probably due to the Li K edge. Local field effects (LFE), which result from microscopic fields induced in the material by the exterior perturbation and from the inhomogeneities of the electronic density of the material,[35] are not included in our calculations. Although these effects were shown to be small on the Li K edge,[36] they are expected to be quite large in the case of the transition metal $M_{2,3}$ edges.[37, 38] This is the reason why the peak corresponding to the Fe $M_{2,3}$ edge is calculated much too intense [Fig. 4(b)]. LFE tend to decrease peak intensities and to spread this intensity to higher energies.[36, 38] For the Li K-edge in LFP, calculated peaks situated at 59.0(2), 60.4(2) and 64.0(2) eV would then, with LFE, be shifted to higher energies (closer to experimental energies). Due to the influence of the superimposed Fe $M_{2,3}$ edge, intensities would also be modified and increased for high

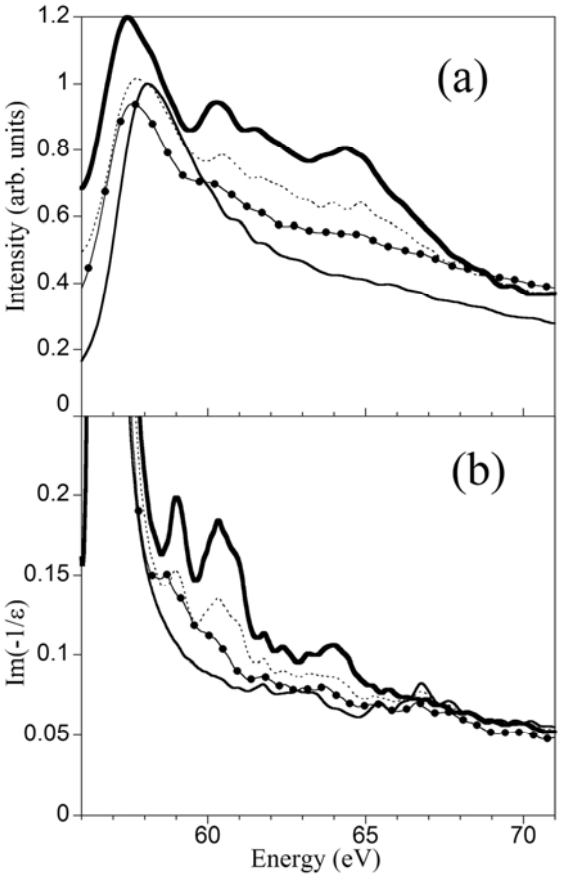

FIG. 4. (a) Experimental Fe-M and Li-K edges spectra. Background subtracted. (b) calculated Fe-M and Li-K edges spectra. Background subtracted and shifted according to Fig 1 shifts. Thick line: $LiFePO_4$; dashed line: two-phases; thin line with dots: single phase; thin line: $FePO_4$.

energies relatively to lower ones. Even if further calculations are necessary, general features are reproduced well enough to allow an analysis of the spectra obtained for single and two-phases samples. In the case of the two-phases sample [dashed line in Fig. 4(a)], the experimental spectrum is intermediate between those of FP and LFP (especially for the peaks situated at 60.3, 61.6 and 64.3 eV). This was expected from the corresponding simulation [dashed line in Fig. 4(b)], which is obtained by averaging FP and LFP calculations. Even if the spectrum for the single phase is not completely featureless from 58 to 68 eV, hardly any peaks are observed in this region. Our calculation for the $Li_{0.5}FePO_4$ structure corresponds very well with this loss of peaks showing that, even if the FP and the LFP atomic structures are closely related, the single phase electronic structure is not a simple average of FP and LFP ones. The difference appears small but is quite reproducible. Fine structures in the Li K edge region can thus give clues on the chemistry of the intercalation in this compound like in others.[39] However, in the prospect of quickly determining phases in Li_xFePO_4 samples via energy filtered images, the Fe $M_{2,3}$ /Li K edge region is clearly not an optimum choice.

In conclusion, using first principles calculations, the most characteristic features in the low loss spectra of LFP and FP were identified. In particular, the area between 3 and 7 eV was shown to be ideal for a fast, unambiguous and easy determination of the repartition of both phases in a sample. For single phase Li_xFePO_4 samples, this 3-7 eV area could be used to quantify the lithium content. In order to distinguish between single and two-phases region, the best choice was however shown to be the careful recording of Li K / Fe $M_{2,3}$ edges. Improved interpretations of the reveled features are expected after inclusion of LFE in the calculations.

ACKNOWLEDGMENTS

We thank J. Gaubicher (IMN) and W. Porcher (CEA) for supplying the starting $LiFePO_4$ materials. The computations presented in this work were performed at the "Centre Régional de Calcul Intensif des Pays de la Loire" financed by the French Research Ministry, the "Région Pays de la Loire", and the University of Nantes.

References

[1] J. M. Tarascon and M. Armand, Nature **414**, 359 (2001).

[2] L. Laffont, C. Delacourt, P. Gibot, M. Y. Wu, P. Kooyman, C. Masquelier, and J. M. Tarascon, Chem. Mater. **18**, 5520 (2006).

[3] A. Yamada, H. Koizumi, N. Sonoyama, and R. Kanno, Electrochem. Solid-State Lett. **8**, A409 (2005).

[4] C. Delmas, M. Maccario, L. Croguennec, F. Le Cras, and F. Weill, Nature Materials **7**, 665 (2008).

[5] N. Meethong, Y.-H. Kao, M. Tang, H.-Y. Huang, W. C. Carter, and Y.-M. Chiang, Chem. Mater. **20**, 6189 (2008).

[6] S.-Y. Chung, S.-Y. Choi, T. Yamamoto, and Y. Ikuhara, Phys. Rev. Lett. **100**, 125502 (2008).

[7] Y. Shao-Horn, S. Levasseur, F. Weill, and C. Delmas, J. Electrochem. Soc. **150**, A366 (2003).

[8] H. Gabrisch, R. Yazami, and B. Fultz, J. Electrochem. Soc. **151**, A891 (2004).

[9] H. Gabrisch, T. Yi, and R. Yazami, Electrochem. Solid-State Lett. **11**, A119 (2008).

[10] G. Chen, X. Song, and T. J. Richardson, Electrochem. Solid-State Lett. **9**, A295 (2006).

[11] M. Kinyanjui, A. Chuvilin, U. Kaiser, P. Axmann, and M. Wohlfahrt-Mehrens, in *14th European Microscopy Congress*, edited by M. Luysberg, K. Tillmann and T. Weirich (Springer, Aachen, Germany, 2008), p. 127.

[12] J. Graetz, C. C. Ahn, R. Yazami, and B. Fultz, J. Phys. Chem. B **107**, 2887 (2003).

[13] S. Miao, M. Kocher, P. Rez, B. Fultz, Y. Ozawa, R. Yazami, and C. C. Ahn, J. Phys. Chem. B **109**, 23473 (2005).

[14] S. Miao, M. Kocher, P. Rez, B. Fultz, R. Yazami, and C. C. Ahn, J. Phys. Chem. A **111**, 4242 (2007).

[15] DigitaMicrograph, (Gatan Inc., Pleasanton, USA, 2003).

[16] P. Blaha, K. Schwarz, G. K. H. Madsen, D. Kvaniscka, and J. Luitz, *WIEN2k, An Augmented Plane Wave + Local Orbitals Program for Calculating Crystal Properties* (Schwarz K., Techn. Universität Wien, Austria, 2001).

[17] F. Zhou, K. Kang, T. Maxisch, G. Ceder, and D. Morgan, Solid State Comm. **132**, 181 (2004).

[18] C. Ambrosch-Draxl, J. A. Majewski, P. Vogl, and G. Leising, Phys. Rev. B **51**, 9668 (1995).

[19] C. Delacourt, J. Rodríguez-Carvajal, B. Schmitt, J.-M. Tarascon, and C. Masquelier, Solid State Sciences **7**, 1506 (2005).

[20] $P2_1ma$ AF space group: $LiFePO_4$: a=10.3377 Å, b=6.0112 Å, c=4.6950 Å, $FePO_4$: a=9.7599 Å, b=5.7519 Å, c=4.7560 Å. 40 irreducible K-points for SCF (4, 7, 9) grid and 252 irreducible K-points for Optic (8, 13, 17) grid. $R_{MT}\times K_{max}=7.5$.

[21] C. Delacourt, P. Poizot, J.-M. Tarascon, and C. Masquelier, Nat Mater **4**, 254 (2005).

[22] S. Franger, C. Bourbon, and F. L. Cras, J. Electrochem. Soc. **151**, A1024 (2004).

[23] A. Gloter, A. Douiri, M. Tencé, and C. Colliex, Ultramicroscopy **96**, 385 (2003).

[24] P. Fallon and C. A. Walsh, University of Cambridge, England (1996).

[25] T. Stöckli, J.-M. Bonard, A. Châtelain, Z. L. Wang, and P. Stadelmann, Phys. Rev. B **61**, 5751 (2000).

[26] H. G. Wessjohann, Phys. Stat. Sol. B **77**, 535 (1976).

[27] P. Moreau and M. C. Cheynet, Ultramicroscopy **94**, 293 (2003).

[28] R. F. Egerton, *Electron Energy-Loss Spectroscopy in the Electron Microscope* (Plenum Press, New York, 1996).

[29] M. Launay, F. Boucher, and P. Moreau, Phys. Rev. B **69**, 035101(1) (2004).

[30] R. O. Jones and O. Gunnarsson, Rev. Mod. Phys. **61**, 689 (1989).

[31] L. Laffont, M. Monthioux, and V. Serin, Carbon **40**, 767 (2002).

[32] J. M. Howe and V. P. Oleshko, J Electron Microsc. (Tokyo) **53**, 339 (2004).

[33] G. Kresse and J. Furthmüller, Phys. Rev. B **54**, 11169 (1996).

[34] space group P11a, a= 10.1300 Å, b=5.9595 Å, c=4.7901Å, g=90°, Li (0,¼,0.7527); Fe^{III} (0.2754,0.9697,0.7238); Fe^{II} (0.2188,0.4814,0.2182); P1(0.0950,0.9799,0.1647); P2(0.4021,0.4717,0.6744); O1(0.1129,0.9896,0.4819); O2(0.3955,0.4598,0.9917); O3(0.4486,0.9786,0.9208); O4(0.0433,0.4716,0.4397); O5(0.1743,0.7837,0.0274); O6(0.6623,0.18330.9940). 70 irreducible K-points for SCF , (4,7,9) K-point grid and 468 irreducible K-points for Optic, (8,13,17) K-point grid.

[35] W. Hanke, Adv. Phys. **27**, 287 (1978).

[36] V. Mauchamp, P. Moreau, G. Ouvrard, and F. Boucher, Phys. Rev. B **77**, 045117 (2008).

[37] F. Aryasetiawan, G. Gunnarsson, M. Knupfer, and J. Fink, Phys. Rev. B **50**, 7311 (1994).

[38] N. Vast, L. Reining, V. Olevano, P. Schattschneider, and B. Jouffrey, Phys. Rev. Lett. **88**, 037601 (2002).

[39] V. Mauchamp, P. Moreau, L. Monconduit, M.-L. Doublet, F. Boucher, and G. Ouvrard, J. Phys. Chem. C **111**, 3996 (2007).